



## *Areospora rohanae* n.gen. n.sp. (Microsporidia; Areosporiidae n. fam.) elicits multi-nucleate giant-cell formation in southern king crab (*Lithodes santolla*)



G.D. Stentiford <sup>a,\*</sup>, K.S. Bateman <sup>a</sup>, S.W. Feist <sup>a</sup>, S. Oyarzún <sup>c</sup>, J.C. Uribe <sup>b</sup>, M. Palacios <sup>c</sup>, D.M. Stone <sup>a</sup>

<sup>a</sup> European Union Reference Laboratory for Crustacean Disease, Centre for Environment, Fisheries and Aquaculture Science (Cefas), Weymouth Laboratory, Weymouth, Dorset DT4 8UB, United Kingdom

<sup>b</sup> Instituto de la Patagonia, Universidad de Magallanes, P.O. Box 113-D, Punta Arenas, Chile

<sup>c</sup> Departamento de Ciencias y Recursos Naturales, Facultad de Ciencias, Universidad de Magallanes, P.O. Box 113-D, Punta Arenas, Chile

### ARTICLE INFO

#### Article history:

Received 31 August 2013

Accepted 13 February 2014

Available online 21 February 2014

#### Keywords:

Xenoma

Synctium

Phylogenetics

Pathogenesis

Taxonomy

Crab fishery

### ABSTRACT

This paper utilises histological, ultrastructure and molecular phylogenetic data to describe a novel genus and species (*Areospora rohanae* n.gen., n.sp.) within the phylum Microsporidia. Phylogenetic and morphological distinction from other known lineages within the phylum also provide strong support for erection of a new family (Areosporiidae n. fam) to contain the parasite. Recognised via lesions observed by workers in king crab processing facilities in southern Chile, the parasite elicits giant cell formation in infected crabs. Merogony within haemocytes and fixed phagocytes proceeds apparent fusion of infected cells to produce multinucleate syncitia in which further development of the parasite occurs. Subsequent recruitment of adjacent cells within the haemal spaces of the hepatopancreas, the podocytes of the gill, and particularly in the subcuticular connective tissues, characterises the pathogenesis of *A. rohanae*. In late stages of infection, significant remodelling of the subcuticular tissues corresponds to the clinical lesions observed within processing plants. Sporogony of *A. rohanae* also occurs within the syncytial cytoplasm and culminates in production of bizarre spores, ornamented with distinctive tubular bristles. Spores occur in sets of 8 within a sporophorous vesicle. The description of *A. rohanae* offers considerable insight into the pathogenesis of giant-cell forming Microsporidia, signifies a new lineage of giant-cell forming Microsporidia in marine hosts, and may reflect emergence of a commercially-significant pathogen in the southern ocean *Lithodes santolla* fishery.

Crown Copyright © 2014 Published by Elsevier Inc. All rights reserved.

### 1. Introduction

The Microsporidia are a diverse parasite phylum infecting host groups from all major taxa in all environments. Almost half of the known genera within the phylum infect aquatic animals (Stentiford et al., 2013b). Prevailing phylogenetic evidence provides strong support for placement of Microsporidians as divergent fungi rather than protists (Capella-Gutiérrez et al., 2012). Hypertrophy of colonised host cells is a well-recognised feature in microsporidium parasitism. In fact, the potential to elicit formation of so-called 'xenoparasitic complexes' is widely reported in the literature and implicates not only the phylum Microsporidia, but pathogens belonging to several protist and metazoan taxa (for review see Lom and Dykova, 2005). Although host cell re-modelling is a common feature of intracellular pathogen infection, Lom and

Dykova (2005) note that in microsporidium infections, the 'xenoma' (describing the xenoparasitic complexes caused by microsporidium infection, after Weissenberg, 1949) are distinct from those formed in other parasitic infections in that the whole microsporidium life cycle takes place within the xenoma. In other parasitic taxa, the xenoparasitic complex usually harbours just one phase of the parasite life cycle. They define the xenoma as '...(the) host cell with a completely changed structure and parasites proliferating inside it, both components being morphologically and physiologically integrated to form a separate entity with its own development in the host at the expense of which it grows'.

Xenoma formation during microsporidium parasitism has been reported in many host taxa and in diverse organ and tissue types. Examples include infections of nervous tissue (e.g. *Spraguea lophii* infections in anglerfish *Lophius piscatorius*; Mrázek, 1899), testis (*Microsporidium cotti* infections in bullhead *Taurulus bubalis*; Chatton and Courrier, 1923), adipose tissue (*Mrazekia argoisi* infection in the isopod *Asellus aquaticus*; Debaisieux, 1931) connective

\* Corresponding author. Fax: +44 0 1305 206601.

E-mail address: [grant.stentiford@cefas.co.uk](mailto:grant.stentiford@cefas.co.uk) (G.D. Stentiford).

tissues (*Desmozoon lepeophtherii* infection in the copepod *Lepeophtheirus salmonis*; Freeman et al., 2003) and the musculature (*Tetramicra brevifilum* infecting turbot *Scophthalmus maximus*; Matthews and Matthews, 1980). Lom and Dykova (2005) also highlight cases of so-called 'syncytial xenoma' formation. An example is *Microsporidium chaetogastris* Schröder, 1909 which elicits the formation of hypertrophic and multinucleate cells of up to 100 µm in diameter in connective and muscle cells of the annelid *Chaetogaster diaphanous*. Here, although the terminology of Lom and Dykova (2005) suggest formation of a syncitium (a multinucleate cell resulting from fusion of adjacent host cells), it cannot be conclusively demonstrated that the giant cells are not in fact a type of 'coenocyte' (multinucleate cell resulting from multiple nuclear divisions without accompanying cytokinesis). In addition, Lom and Dykova (2005) note that in some cases 'amitotic' division of host cell nuclei into nuclear fragments may lead to formation of a network of nuclei at the periphery of the giant cell.

Regardless of specific pathogenic mechanisms within the host cell, well-studied xenoma forming Microsporidia such as *Glugea* spp. (infecting fish) have led to proposals that host cells within the blood lineage (e.g. macrophages, neutrophils) likely provide the mechanism by which infective life stages are transported from the gut to the site of giant cell formation (e.g. Sánchez et al., 2001). In the case of *Loma salmonae*, merogony is initiated within the circulating blood cells, a feature also reported in *T. brevifilum* (Matthews and Matthews, 1980). The process beyond this point is less clear – with either the target cell (e.g. gill epithelia) phagocytising the vector cell and converting itself into the xenoma, or by some mechanism whereby the vector cell itself forms the xenoma (see Rodríguez-Tovar et al., 2003; Lom and Dykova, 2005). Research focused on giant-cell development using *in vitro* models of microsporidium parasitism (*Vittaforma corneae*) have demonstrated formation of large (up to 200 µm), multinucleate structures made up of single or multiple fused kidney cells. However, similar structures were not formed when microsporidium infected epithelial cell lines (Leitch et al., 2005). The authors proposed that for giant cell formation to occur, the host cell must be capable of continuous mitosis and not be terminally differentiated. Such data provide useful insights into the potential host cell origin of xenomas observed infections *in vivo*.

The family Lithodidae (stone or king crabs) is comprised of 16 genera and over 90 species (Donaldson and Byersdorfer, 2005). Within the family, two genera contain representative species exploited in the global fishery; *Lithodes* and *Paralithodes*. Microsporidia have been reported infecting three species of king crab

(*P. camtschaticus*, *P. platypus*, and *L. aequispina*) in the eastern Bering Sea where they are known to cause so-called 'cottage cheese disease' (see Morado, 2011). Although the aetiology has been assigned to an undescribed species of the genus *Thelohania* (Hazard and Oldacre, 1975), more recent work by our laboratory (Stentiford et al., 2013a) has proposed that morphological plasticity precludes taxonomic placement of Microsporidia based purely on ultrastructural features. For this reason, and those outlined in specific studies of the genus *Thelohania* by Brown and Adamson (2006) further research will be required to classify the causative agent of 'cottage cheese disease' in northern king crabs. Although Morado (2011) reports a primary infection site within the hepatopancreas (and occasionally the ovary and skeletal muscles) close scrutiny of the gross pathology and histopathological figures provided therein are suggestive of infection of cells within the haemal spaces of the hepatopancreas (rather than in epithelial cells *per se*), and in sub-cuticular tissues of the abdomen.

Here, we report on the distinctive pathogenesis and taxonomy of a novel giant-cell forming microsporidium pathogen infecting the deep water southern king crab (*Lithodes santolla*) from sub-Antarctic waters off Chile. *L. santolla* supports a valuable fishery between Valdivia in south-central Chile and Cape Horn in the far south of the country. Infected animals, displaying characteristic, externally visible lesions, not dissimilar to those previously reported in king crabs from the Bering Sea, were observed at onshore processing facilities. Morphological, ecological and phylogenetic data, the latter based on partial sequencing of the ssrDNA gene, provided evidence that the microsporidium represented a novel taxon within the phylum Microsporidia. Distinction from existing genera within the phylum provided impetus for erection of a new genus and species (hereby *Areospora rohanae* n.gen. n.sp.) and potentially, a novel family (Areosporiidae n. fam.) of giant-cell forming Microsporidia. It represents the first fully characterised microsporidium infecting the connective tissues of a crustacean host and provides insight into the pathogenesis of giant-cell formation associated with parasites from the phylum Microsporidia.

## 2. Materials and Methods

### 2.1. Field sampling for histology, transmission electron microscopy and molecular diagnostics

Southern king crabs (*L. santolla*) were sampled from the commercial fishery as part of ongoing fisheries surveys in Patagonia, Chile during 2012. Crabs displaying characteristic lesions (white,

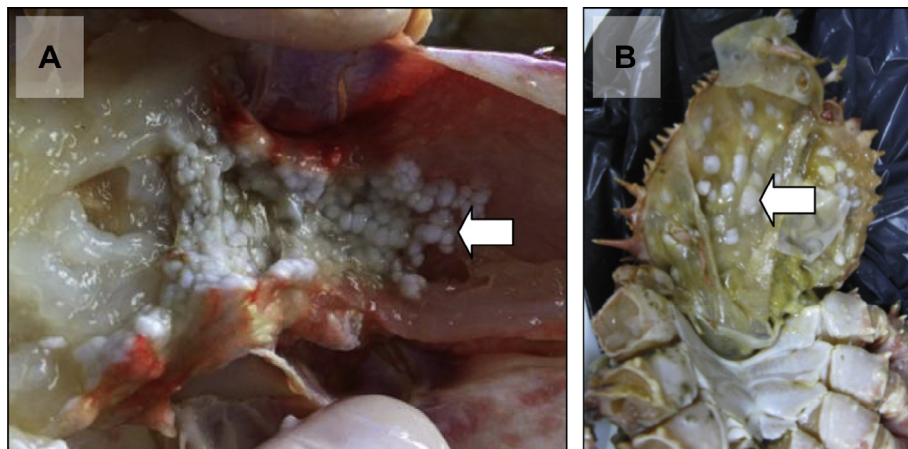


**Fig. 1.** Gross observations of *Areospora rohanae* n.gen., n.sp. in *Lithodes santolla*. (A) Walking limb. White 'xenoma'-like lesions (arrow) are present throughout the soft tissues of the limb. (B) Abdomen. Similar 'xenoma'-like lesions to those observed within the limbs are associated with the sub-cuticular epidermis and underlying connective tissues (arrow).

opaque raised nodules within sub-cuticular tissues) were transferred to the laboratory prior to chilling to 4 °C and processing for histology, electron microscopy and molecular biology. For histology, the distinctive sub-cuticular lesions were sampled along with skeletal musculature, hepatopancreas and gill. Excised samples were placed into Davidson's seawater fixative (Hopwood,

1996) and fixation was allowed to proceed for 24 h before transfer to 70% industrial methylated ethanol. For transmission electron microscopy, sub-cuticular lesions were removed and small blocks of tissue ( $2 \text{ mm}^3$ ) were fixed in 2.5% glutaraldehyde in 0.1 M sodium cacodylate buffer (pH 7.4). For molecular diagnostics, regions containing sub-cuticular lesions were dissected and fixed

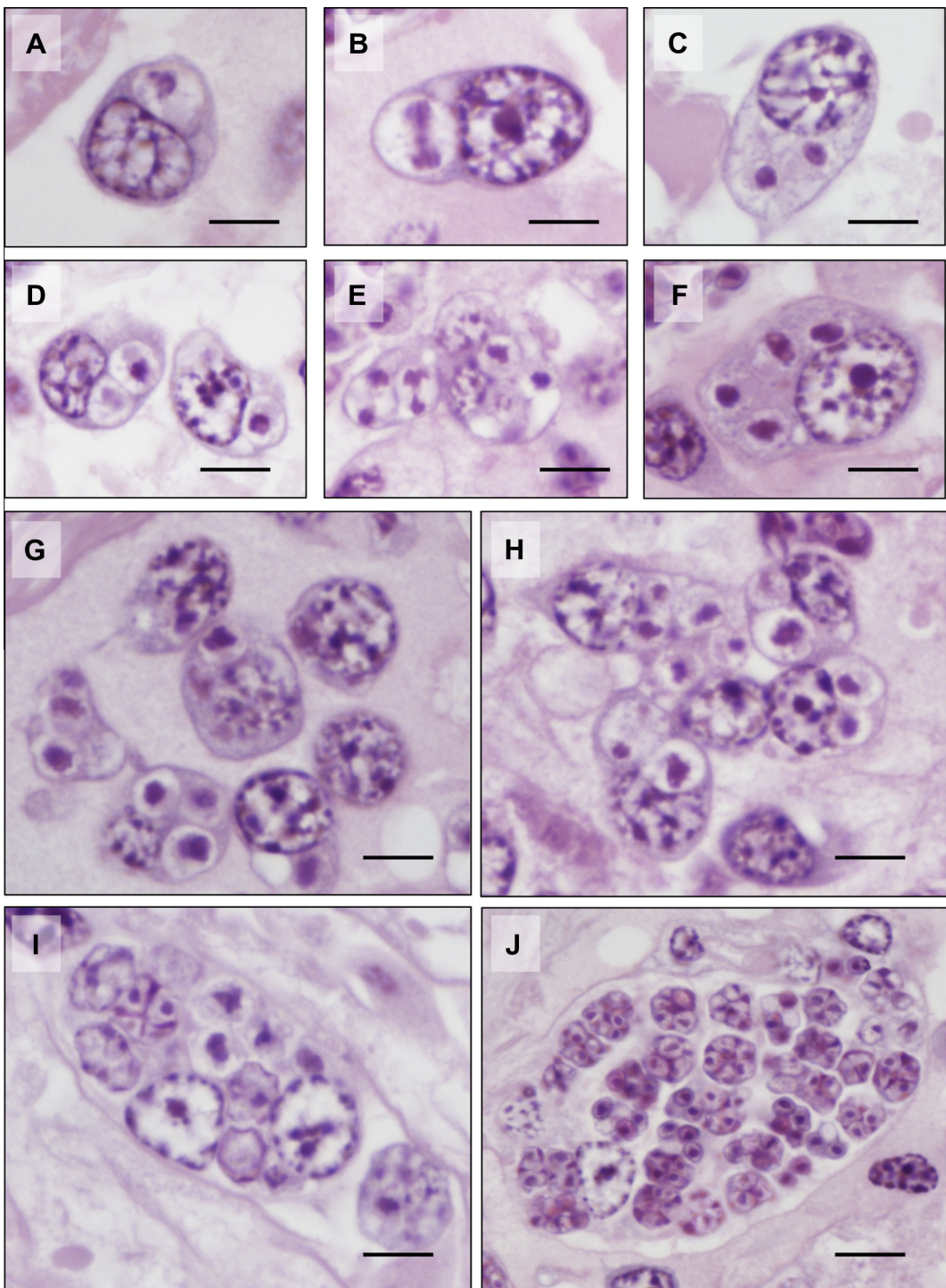


**Fig. 2.** Early infection and merogony of *Areospora rohaneae* n.gen., n.sp. in *Lithodes santolla*. (A) Uninucleate meront within host phagocytic cell. (B) Nuclear division in uninucleate meront. (C) Two uninucleate meronts within phagocyte cytoplasm. (D) Adjacent phagocytes containing one or two uninucleate meronts. (E) Simultaneous division of adjacent uninucleate meronts within the phagocyte cytoplasm. (F) Single phagocyte containing four uninucleate meronts. (G) Several adjacent phagocytes containing merogonal life stages. (H) Apparent fusion of phagocytes to form multinucleate phagocyte syncitium. (I) Early phagocyte syncitium (containing 3 visible host nuclei). The cytoplasm of the syncitium contains parasite life stages at various states of early development. (J) Early sporogony in phagocyte syncitium. All scale bars in 5  $\mu\text{m}$ . All H&E histology.

immediately in 100% ethanol. Samples were dispatched to the European Union Reference Laboratory for Crustacean Diseases, United Kingdom for processing and interpretation.

## 2.2. Histology and transmission electron microscopy

For histology, fixed samples were processed to wax in a vacuum infiltration processor using standard protocols (see Stentiford et al., 2013a). Sections were cut at a thickness of 3–5 µm on a rotary microtome and mounted onto glass slides before staining with H&E (Bancroft and Stevens, 1996). Stained sections were analysed by light microscopy (Nikon Eclipse E800). Digital images and measurements were obtained using the Lucia<sup>TM</sup> Screen Measurement System (Nikon, UK).

For transmission electron microscopy (TEM), fixed samples were rinsed in 0.1 M sodium cacodylate buffer (pH 7.4) and post-fixed for 1 h in 1% osmium tetroxide in 0.1 M sodium cacodylate buffer. Samples were washed in three changes of 0.1 M sodium cacodylate buffer before dehydration through a graded acetone series. Samples were then embedded in epoxy resin 812 (Agar

Scientific-pre-mix kit 812 (Agar Scientific, UK) and polymerised overnight at 60 °C. Semi-thin (1–2 µm) sections were stained with Toluidine Blue for viewing with a light microscope to identify suitable target areas. Ultrathin sections (70–90 nm) of these areas were mounted on uncoated copper grids and stained with uranyl acetate and Reynolds' lead citrate (Reynolds, 1963). Grids were examined using a JEOL JEM 1400 transmission electron microscope and digital images captured using a Gatan Erlangshen ES500W camera and Gatan Digital Micrograph<sup>TM</sup> software.

## 2.3. DNA extraction, PCR and sequencing

Samples corresponding to lesions observed in field, histology and TEM preparations were processed for the partial sequencing of the small subunit ribosomal RNA (SSU rRNA) gene. Tissue samples were weighed and 50–100 mg added to Lysing Matrix D Fast-Prep<sup>®</sup> tubes followed by dilution in G2 buffer and proteinase K (Qiagen) to give 10% weight/volume. Following disruption of the tissues using the FastPrep<sup>®</sup> cell disrupter, homogenates were incubated at 56 °C overnight. Volumes equivalent to 5 mg of tissue

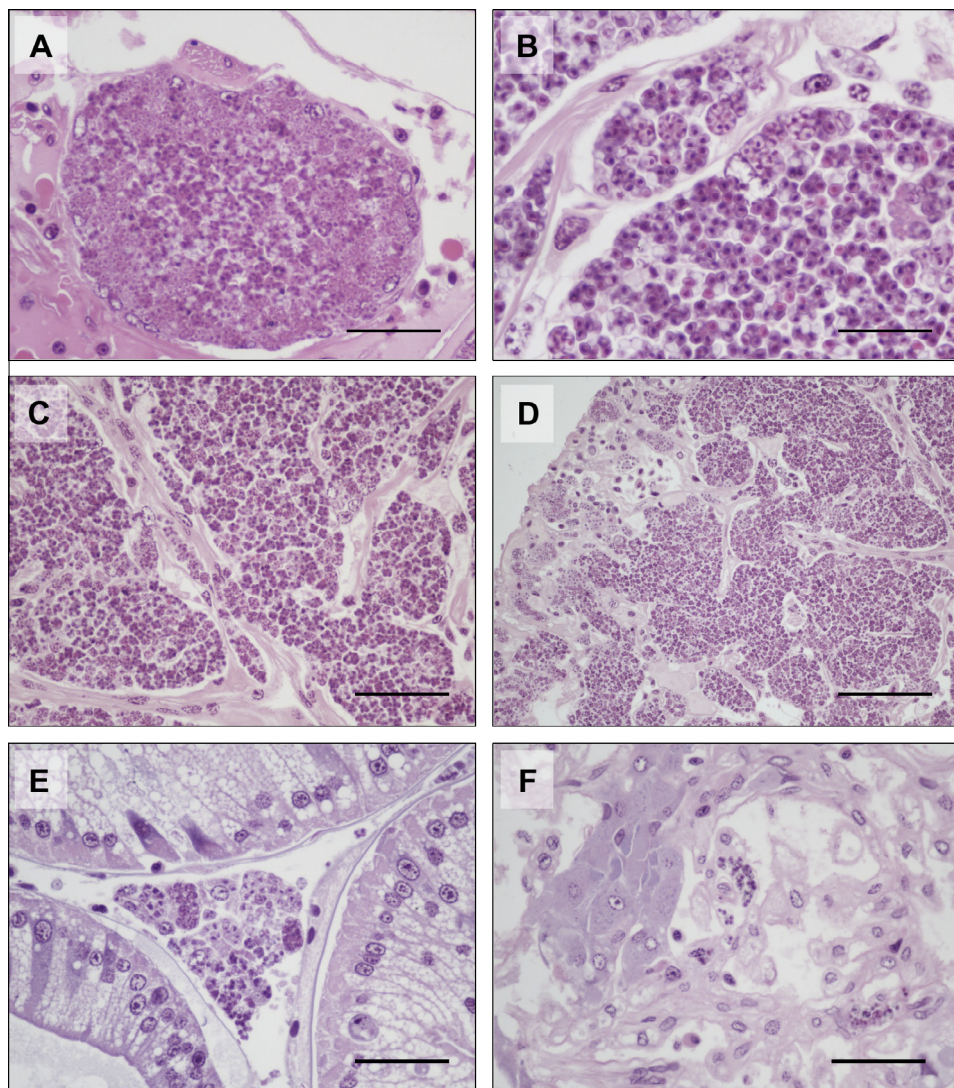


**Fig. 3.** Sporogony and development of disease during *Areospora rohanae* n.gen., n.sp. infection of *Lithodes santolla*. (A) Multinucleate phagocytic syncitium containing maturing parasite stages. Host nuclei are located at the periphery of the syncitium and mature life stages (spores) occur towards the centre. Scale 100 µm. (B) Syncitium containing mature spores. Scale 25 µm. (C and D) Progression of disease involves the apparent fusion of smaller multinucleate syncitia (containing maturing stages and spores) until the majority of the connective tissues are replaced with numerous large syncitia. Scale 100 µm (E, F). Infection also implicates the fixed phagocytes within the haemal spaces of the hepatopancreas (E) and the podocytes within the primary lamellae of the gills (F). Scale 100 µm. All H&E histology.

were removed and DNA extracted using the QIAGEN EZI DNA Tissue Kit and the BioRobot® EZ1. DNA was eluted in a 50 µl volume. PCR reactions were performed in a 50 µl reaction volume consisting of 1× GoTaq flexi buffer (Promega, UK), 2.5 mM MgCl<sub>2</sub>, 1 mM dNTP mix, 50 pmol each of the MF1 primer and MR1 primer (Tourtip et al., 2009), 1.25 units of GoTaq DNA Polymerase (Promega, UK) and 2.5 l of the purified DNA. The reaction mix was overlaid with mineral oil and after an initial denaturing step (5 min at 95 °C), was subjected to 35 temperature cycles (1 min at 95 °C, 1 min at 55 °C and 1 min at 72 °C) in a Peltier PTC-225 thermal cycler followed by a final extension step of 10 min at 72 °C. PCR products were visualised on 1.5% agarose gels stained with ethidium bromide. PCR products were purified using the Freeze N' Squeeze DNA purification system (Anachem, UK) and both DNA strands were sequenced using the same primers used for the amplification. The partial SSU rRNA gene of 2 independent samples were amplified and sequenced in duplicate and the resulting consensus sequences were submitted to GenBank (to be assigned).

#### 2.4. Phylogenetic analysis

Multiple sequence alignments and phylogenetic analysis was performed using the 908 nucleotide partial SSU rRNA gene sequence from the crab parasite and the equivalent region of the SSU from a wide range of microsporidium species. Partial SSU rRNA gene sequences from *Basidiobolus ranarum* (AY635841) and *Conidiobolus coronatus* (AF296753) were used as an outgroup. Multiple alignments were performed using Clustal W (Thompson et al., 1997) using the following Clustal parameters: a gap opening penalty of 15, and gap extension penalty of 6.66. Phylogenetic analyses were conducted using MEGA version 4 (Tamura et al., 2007). The neighbour-joining tree was constructed using a maximum composite likelihood model and the robustness of the tree was tested using 1000 bootstrap replicates. The maximum parsimony trees were constructed using the unweighted parsimony method described in Fitch (1971), and again, the robustness of the tree was tested using 1000 bootstrap replicates.

### 3. Results

#### 3.1. Field observations

*L. santolla* displaying clinical signs of infection were initially observed within processing plants for this highly valuable fishery species. They were recognised by the presence of large, white/opaque and raised lesions, most visible within the joints of walking limbs (Fig. 1a) and in the soft, sub-cuticular tissues of the abdomen (Fig. 1b). The lesions resembled xenomas caused by infection with Microsporidia of the genus *Spraguea* spp. in the nervous system of anglerfish, and *Glugea* spp. in the viscera of numerous marine teleosts (for both, see Lom and Dykova, 2005). Whilst it was not possible to ascertain the precise tissue type containing these lesions, the skeletal musculature was not apparently implicated.

#### 3.2. Histopathology

Histology of crabs displaying externally-visible clinical signs revealed a progressive colonisation of the sub-cuticular connective tissues with a highly proliferative intracellular pathogen. Since all of the crabs observed were in an advanced stage of disease and significant tissue remodelling had occurred at the time of sampling, the identity of infected cell types was not obvious. However, since foci of infection were detected in the connective tissues of walking limbs, within the primary stem of gill lamellae and within the hepatopancreatic haemal sinuses, it was assumed that the primary

infection sites were haemocytes and phagocyte clusters (PC). Whilst massive colonisation of the sub-cuticular connective tissues appeared to follow initial infection of the PCs, whether subsequent auto-infection implicated the spongy connective tissue cells, reserve inclusion cells, fibroblasts and haemocytes is uncertain.

Early infections of PCs were observed as apparent uninucleate life stages within the PC cytoplasm (Fig. 2A). Nuclear fission (Fig. 2B) led to the presence of two (Fig. 2C and D) and four (Fig. 2E and F) discrete parasites within the PC cytoplasm. Aggregation of infected PCs (Fig. 2G) caused formation of a distinctive syncitium (Fig. 2H) in which multiple host nuclei could be observed amongst developing parasite life stages (Fig. 2I). Subsequent development of early life stages of the parasite into rosette-like clusters occurred within the cytoplasm of the multi-nucleate host cell syncitium (Fig. 2J). Presumed recruitment of adjacent syncitia, with simultaneous development of parasite life stages within the syncytial cytoplasm initiated a progressive remodelling of the connective tissue matrix until the majority of the tissue mass was replaced with parasite-filled multinucleated giant cells (Figs. 3A–C). Giant syncitia were separated by fibrous remnants of the connective tissue matrix but epithelial cells of the subcutis were not implicated (Fig. 3D). Similarly, aforementioned colonisation of the PCs within the hepatopancreatic haemal sinuses (Fig. 3E) and the podocytes of the gill (Fig. 3F) did not progress to infection of the either the hepatopancreatic tubules epithelia, or gill epithelia, respectively.

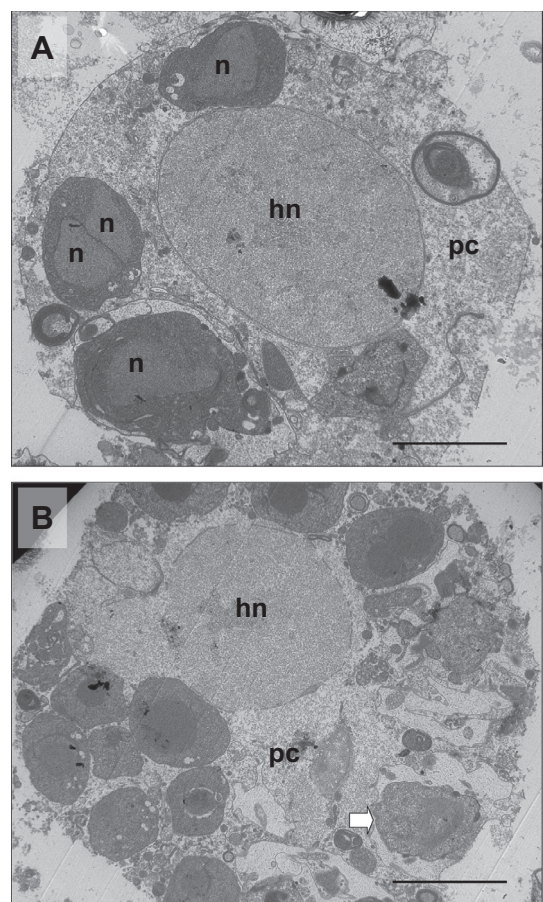


**Fig. 4.** (A and B) Low power ultramicrographs showing infection of phagocytes of *Lithodes santolla* by potentially uninucleate (n) and diplokaryotic meront (n/n) life stages of *Areospora rohaneae* n.gen., n.sp. The host nucleus (hn) is enlarged and the host cell cytoplasm (pc) appears degenerate. In some cases, uninucleate life stages were apparently contained at the periphery of the phagocyte within a phagocytic vacuole (arrow). Scale 2 µm. Transmission electron microscopy.

### 3.3. Ultrastructure

Crabs displaying clinical signs and histopathological lesions were shown to be infected with a novel microsporidium parasite. Ultrastructural observations of infected tissues revealed merogonic and sporogonic life stages which culminated in the production of bizarre spores, ornamented with distinctive tubular bristles emerging from the exosporal layer. The earliest life stages, detected within the cytoplasm of apparent PCs, were possibly uninucleate and confirmed diplokaryotic meronts (Figs. 4A and B). Some of the electron-dense meronts were apparently contained within vacuoles whilst others lay in direct contact with the PC cytoplasm (see Fig. 4B) Since multiple meronts occurred within the cytoplasm of individual PCs, some presumably emerged from division (see histology in Fig. 2A–F) whilst others came from multiple phagocytic events by previously infected cells. Late merogony was depicted by a progressive arrangement of nuclear and cytoplasmic elements of the parasite within a limiting membrane, presumably of parasite origin (sporophorous vesicle, SPV) within which all subsequent stages of parasite sporulation occurred (Fig. 5A and B). At this stage, electron dense accumulations occurred at the periphery of the sporont wall. Development of tubular bristles progressively colonised the space between the parasite and the SPV wall (Fig. 5C–E). The initiation of sporogony was marked by the forma-

tion of septa between isolated nuclei and the progressive thickening of the septa to form the pre-sporont wall (Fig. 5F). A distinctive rosette-like structure, bound within the SPV, was observed in early sporogony (Fig. 6A). This stage likely corresponded to similarly observed structures within infected host cell syncitia via histology (see Fig. 2J). Normally, five lobes of the rosette were visible in section, although it was presumed that such rosettes were comprised of 8 pre-sporonts (the remainder occurring out of section) (Fig. 6B). The transition of rosette-like sporonts to early sporoblasts was marked by the formation of the spore-extrusion precursors (e.g. the polar filament) and the apparent migration of tubular bristles to the surface of the pre-sporont exospore layer (Fig. 6C). All observed sporoblast stages were uninucleate (Fig. 6D). Maturation of sporoblasts was marked by the gradual ordering of spore organelles (Fig. 6E), thickening of the endospore and appearance of a distinctive multi-layered exospore into which the tubular bristles were apparently inserted (Fig. 6F). Uninucleate mature spores measured  $2.8 \mu\text{m} \times 2.2 \mu\text{m}$  and occurred in sets of 8 within an SPV (Fig. 7A and inset). The polar filament was isofilar and coiled 10–11 times, in two disorganized layers (Fig. 7B). The polar filament terminated at an anchoring disk after passing through a laminar polaroplast. The exospore was multi-layered and ornamented with a dense covering of tubular bristles which appeared to be rooted within the endosporal layer (Fig. 7C). A putative life

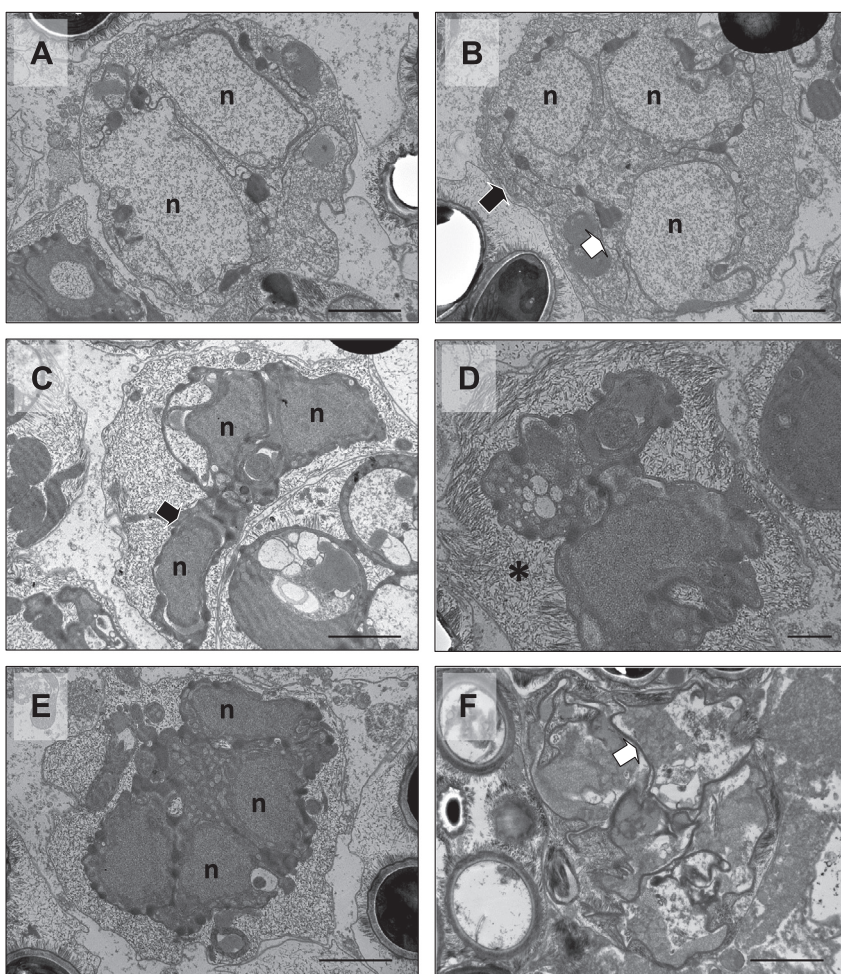


**Fig. 5.** Early sporogony of *Areospora rohanae* n.gen. n.sp. in *Lithodes santolla*. (A) Apparently binucleate (n) meront Scale 2  $\mu\text{m}$ . (B) Tetranucleate meront (three nuclei visible, n) and formation of the sporont wall (white arrow) within the sporophorous vesicle (black arrow) – the latter corresponding to the meront wall. Scale 2  $\mu\text{m}$ . (C) Early maturation of the sporont involves increasing electron density within the confines of the sporont wall (black arrow) and of the nuclei (n). Scale 2  $\mu\text{m}$ . (D) Further maturation of the sporont, with the first appearance of tubular bristles in the region between the sporont wall and the SPV wall (asterisk). Scale 500 nm. (E) Maturing sporonts arrange into an early rosette structure (four nuclei visible, n) Scale 500 nm. (F) Late sporogony depicted by thickening of the wall separating individual nuclei within sporont sac (arrow). Scale 500 nm. All transmission electron microscopy.

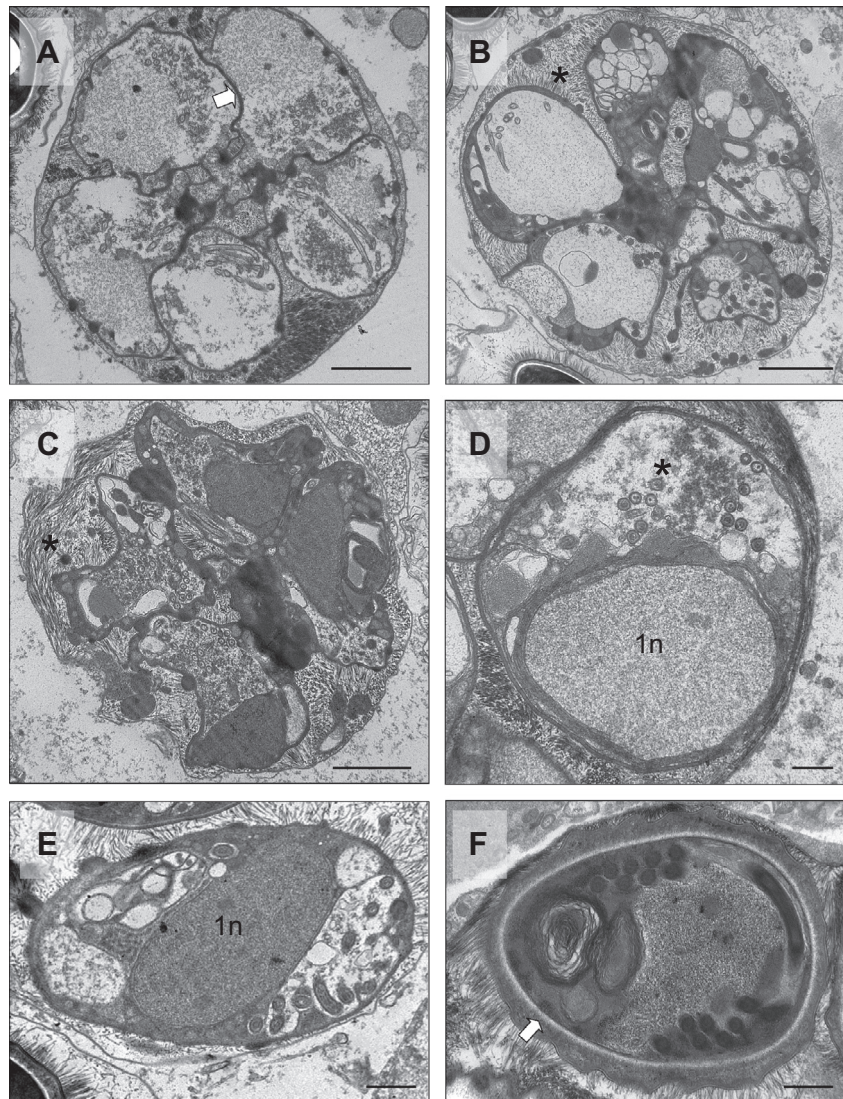


**Fig. 6.** Sporoblast production of *Areospora rohanae* n.gen. n.sp. in *Lithodes santolla*. (A) Individual SPV in late sporogony. Early sporoblasts arrange in a rosette and are separated by an electron dense plasmalemma (arrow). Scale 2 μm. (B) Maturing SPV showing increasing separation of pre-sporoblasts and early production of tubular bristles within space between pre-sporoblasts and SPV wall (asterisk). Scale 2 μm. (C) Maturing SPV with further distinction of individual early sporoblasts and development of bristles (asterisk). Scale 2 μm. (D) Immature sporoblast with prominent nucleus (1n) and early formation of polar filament (asterisk). Scale 500 nm. (E) Immature sporoblast with central nucleus (1n) and bristles visible at the surface of the spore. Thickened endospore layer not yet present. Scale 500 nm. (F) Mature sporoblast with thickened endospore (arrow) and ornamented spore wall. Scale 500 nm. All transmission electron microscopy.

cycle of the microsporidium parasite based upon observed life stages is provided in Fig. 8.

#### 3.4. Molecular phylogeny

The 948 nucleotide partial SSU rRNA gene sequence obtained for the microsporidium parasite in *L. santolla* shared a maximum of 67% nucleotide identity with the SSU of *Janacekia debaisieuxi* (AY090070) over a 852 nucleotide region, and 66% nucleotide identity with the SSU of both *Hamiltosporidium tvaermannensis* (GQ843833) and *H. magnivora* (AY649786) over a 722 nucleotide region. Distinction of the partial SSU rRNA gene sequence and morphological differences to all known genera (see Section 3.5) of Microsporidia provided evidence for erection of a new genus and species (*A. rohanae*). *A. rohanae* n.gen., n.sp. branches from the main clades (of Vossbrinck and Debrunner-Vossbrinck, 2005) together with *H. magnivora* (AY649786), but this separation was supported by boot strap values of <55%, suggesting that both *A. rohanae* and *H. magnivora* (AY649786) represent distinct lineages

within the phylum Microsporidia (Fig. 9). The distinct lineage containing *A. rohanae* may also be used to erect a new family within the phylum Microsporidia; as such, *Areosporiidae* n. fam. is proposed.

#### 3.5. Taxonomic description

##### Phylum Microsporidia Balbiani, 1882.

Class Marinospordia Vossbrinck and Debrunner-Vossbrinck, 2005.

##### Family Areosporiidae (proposed, this study).

Erection of the family is proposed based upon distinction of the parasite described herein from all other known families within the phylum (using partial sequence data for the ssrRNA gene). Morphological features of the new (monotypic) family are as described in generic and species descriptions (below). Strict morphological definition of the family is not possible due to potential for discovery novel, morphological variants and the well documented potential for plasticity in closely related microporidium taxa.

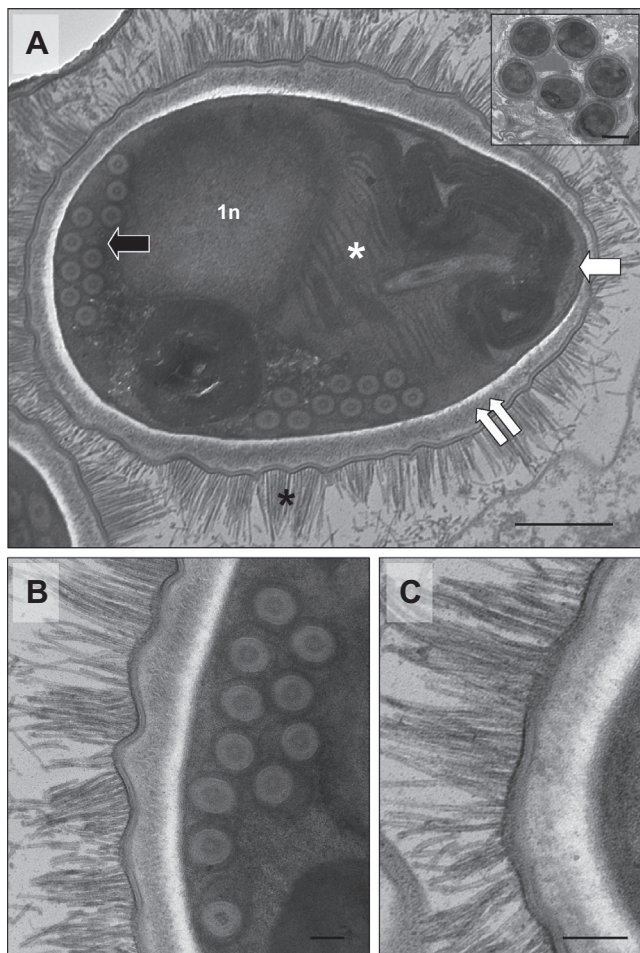


**Fig. 7.** Mature spore of *Areospora rohanae* n.gen., n.sp. in *Lithodes santolla*. (A) Individual uninucleate (1n) spore with 10 turns of an isofilar polar filament (black arrow) terminating at the anchoring disk (white arrow) after passing through the laminar polaroplast (white asterisk). The thickened endospore (double white arrows) is surrounded by a laminar exospore ornamented in bristles (black asterisk). Scale 500 nm. (Inset shows individual sporophorous vesicle containing 8 spores; Scale 2 μm). (B) Detail of isofilar polar filament arranged in two ranks at the spore periphery. Scale 100 nm. (C) Detail of tubular bristles ornamenting the surface of the exospore. Scale 100 nm. All transmission electron microscopy.

#### Genus *Areospora* n. gen.

**Definition.** Merogonic and sporogonic stages occur within the cytoplasm of phagocytes and connective tissue cells of marine crustacean hosts. Parasite life stages may be bound within an SPV. Early sporogony defined by distinctive rosette-like structure, bound within a SPV. Rosettes comprise 8 pre-sporonts. Transition of rosette-like sporonts to early sporoblasts marked by formation of spore-extrusion precursors and migration of tubular bristles to the surface of the pre-sporoblast exospore layer. Monokaryotic spores, ornamented with distinctive bristles. Distinction from other known genera within the phylum based upon partial sequence of the ssrRNA gene.

#### *A. rohanae* n.sp.

**Specific diagnosis:** Merogonic and sporogonic stages corresponding to the generic description for *Areospora* n. gen., occurring within phagocytes and connective tissue cells of lithodid crabs. Placement within the genus *Areospora* based upon high similarity of partial sequences of the ssrRNA gene. Parasite life stages may be bound within an SPV. Early sporogony defined by distinctive rosette-like structure, bound within a SPV. Rosettes comprise 8 pre-sporonts. Transition of rosette-like sporonts to early spor-

oblasts marked by formation of spore-extrusion precursors and migration of tubular bristles to the surface of the pre-sporoblast exospore layer. Maturation of sporoblasts marked by gradual ordering of spore organelles, thickening of endospore and appearance of distinctive multi-layered exospore into which the tubular bristles are inserted. Monokaryotic spores, ornamented with distinctive bristles in the exosporal layer occur in sets of 8 within a sporophorous vesicle. Uninucleate mature spores measure approximately 2.8 μm × 2.2 μm in specimens fixed for TEM. Spores contain an isofilar polar filament coiled 10–11 times, in two layers. Exospore is multi-layered and ornamented with dense covering of tubular bristles.

**Type host:** *Lithodes santolla* Molina, 1782.

**Type locality:** Straits of Magellan, southern Chile.

**Site of infection:** Cytoplasm of phagocytes and connective tissue cells.

**Etymology:** The generic name refers to site of infection within the connective tissues of the host. The specific epithet is derived from the given name (Rohana) of the daughter of the first author (Stentiford).

**Type material:** Syntype slides of histological sections stained with H&E and transmission electron microscopy blocks have been deposited in the Registry of Aquatic Pathology (RAP) at the Cefas Weymouth Laboratory. The partial sequences of the ssrRNA gene have been deposited in Genbank under accession numbers (to be assigned).

#### 4. Discussion

In this paper, we describe the type genus and species of a novel lineage of microsporidium parasite infecting the phagocytes and connective tissues of *L. santolla*, a commercially-exploited marine crustacean from Chile. The parasite is hereby named *A. rohanae* n.gen., n.sp. and is used to define a new family, the Areosporiidae, within the phylum Microsporidia. Phylogenetic analyses based upon partial sequencing of the SSU rRNA gene revealed very low similarity to all known taxa within the phylum. Whilst the SSU rRNA has limitations for the distinction of species within a genus, it is considered useful for the discrimination of genera (and higher ordering) within the phylum (Vossbrinck and Debrunner-Vossbrinck, 2005). The low nucleotide identity (67%) between the SSU rRNA gene sequence between *A. rohanae* and that of its closest match (*Janacekia debaisieuxi* infecting simulid flies) provided strong support for erection of the new genus. Erection of higher taxonomic groupings (e.g. family) is generally appropriate when comparative morphological and phylogenetic data is available from sufficient numbers of similar taxa (Stentiford et al., 2010, 2011). Although such comparative data is not available in this case, the phylogenetic distinction of *A. rohanae* from existing members of the phylum when coupled with its morphological characteristics may be sufficient for erection of a new family (Areosporiidae n. fam) to contain it. Future descriptions of novel taxa similar to *A. rohanae* are required to provide validity to the erection of this novel family within the phylum. Initially, this should involve phylogenetic studies on the microsporidium causing so-called 'cottage cheese disease' in lithodid crabs from the northern hemisphere (Hazard and Oldacre, 1975; Ryazanova and Eliseikina, 2010; Morado, 2011) and on other Microsporidia with 'Thelohania-like' developmental characteristics in other marine crustaceans (Hazard and Oldacre, 1975). However, in the case of the latter, the well-documented potential for significant morphological plasticity within even closely related Microsporidia suggest that defining relationships based solely on such morphological features, is unlikely (Stentiford et al., 2013a,b).

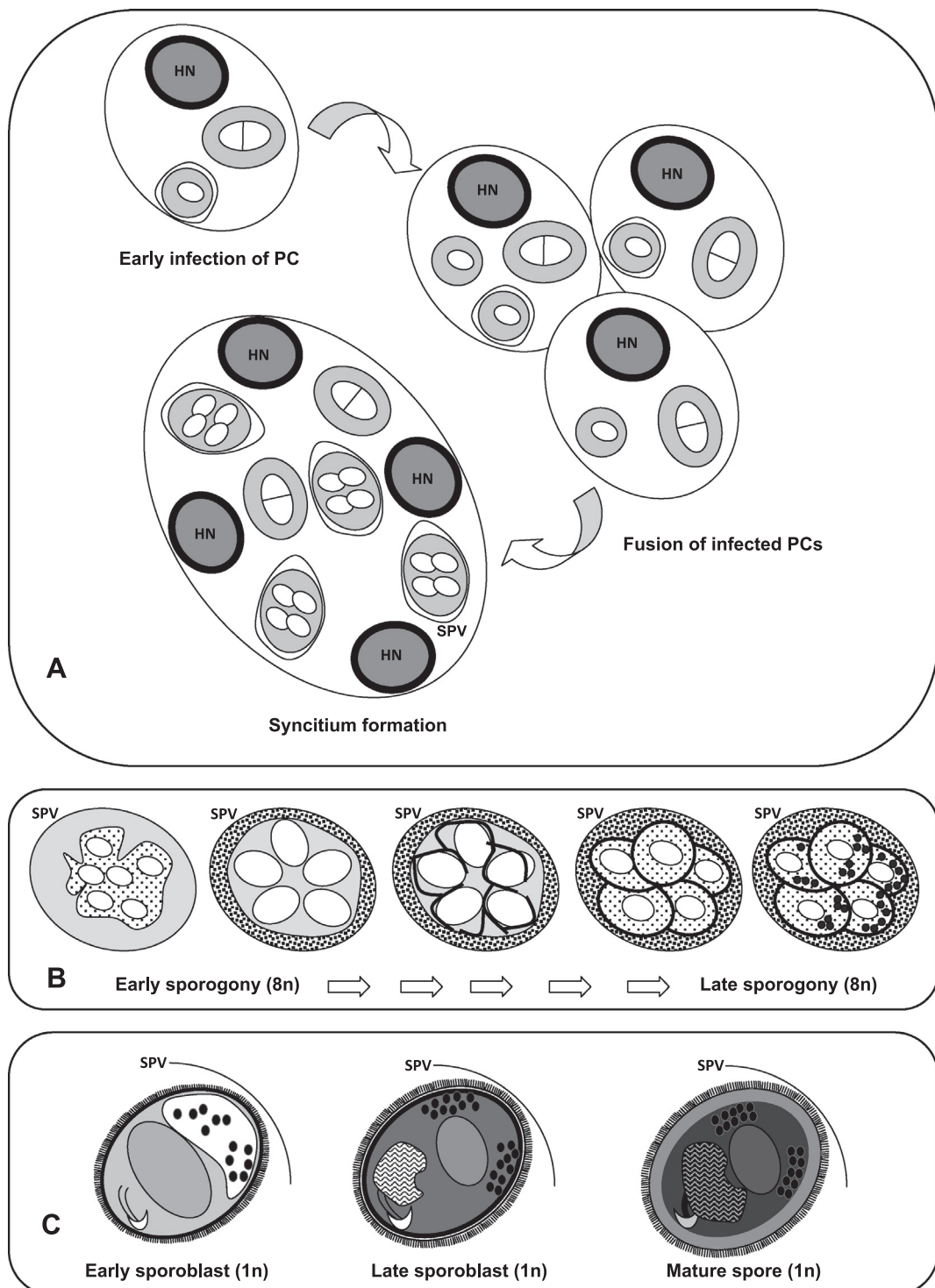


**Fig. 8.** Putative developmental stages of *Areospora rohanae* n.gen., n.sp. in *Lithodes santolla*. Box A: Infection and merogony within uninucleate (HN) host phagocytes (PC) leads to fusion of PCs to form a multinucleate giant cell containing developing stages of the parasite, contained within individual sporophorous vesicles (SPV). Some meronts are initially contained within phagocytic vacuoles but most appear in direct contact with PC cytoplasm. Box B: Merogony to late sporogony, producing 8 uninucleate spores, within individual SPVs in the cytoplasm of giant cells. Box C: Spore maturation (x8) within an individual SPV.

The connective tissues of crustaceans are interstitial tissues of mesodermal origin. Johnson (1980) proposed that two types exist: the fibrous connective tissues, in which fibroblasts form a lattice of fibres which encapsulate tissues, organs and haemolymph vessels; and the spongy connective tissue comprising large vacuolated cells containing glycogen, and reserve inclusion cells (likely containing haemocyanin). Interspersed with the connective tissues are

'rosettes' of fixed phagocytes applied to the walls of the arterioles (Johnson, 1980). Although several descriptions of Microsporidia have stated infection of 'connective tissues' associated with specific organs (e.g. Wang et al., 2013), it is informative to consider the specific cell types within these mixed cell populations that can become infected. The pathogenesis of *A. rohanae* appears to offer considerable insight into connective tissue infections in

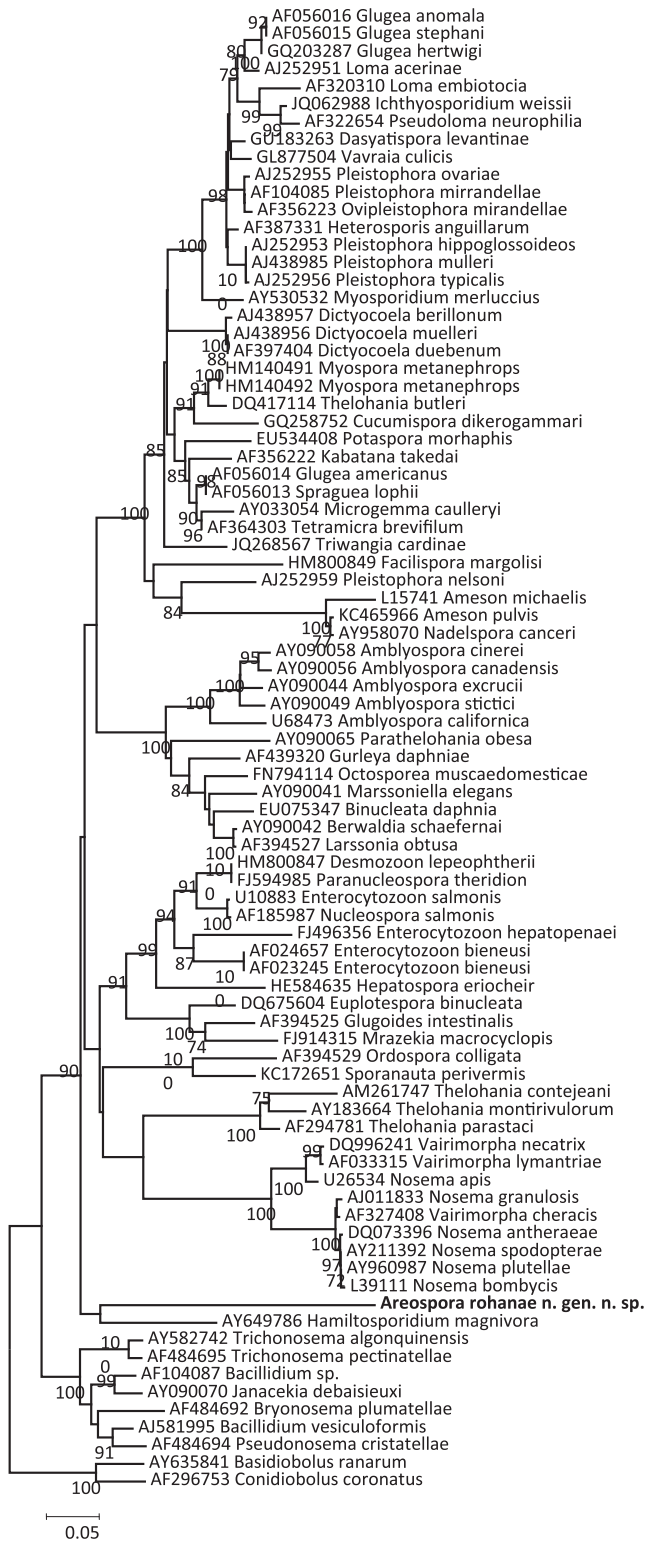


**Fig. 9.** Neighbour-joining tree based on a 948 nucleotide partial SSU rRNA gene sequences of *Areospora rohanae* and the equivalent region of 81 microsporidium species. Partial SSU rRNA gene sequences from *Basidiobolus ranarum* (AY635841) and *Conidiobolus coronatus* (AF296753) were used as an out-group. The phylogenetic analysis was performed using MEGA version 3.1. Analysis was done on 1000 bootstrapped data sets and values of >70% are shown on the tree. The scale bar represents substitutions per nucleotide site.

invertebrates and further, to the process of giant-cell formation associated with microsporidium infections. Detailed histopathology of infected tissues showed that early infections occurred either

within phagocytes (haemocytes) or within rosettes of fixed phagocytes. Fusion of infected phagocytes, either within the gill lamellae, the sinuses of the hepatopancreas, or more commonly in the connective tissues of the subcutis initiated formation of syncitia (multi-nucleated giant cells) containing all developing stages of the parasite. Small syncitia apparently fused to occupy the majority of the subcuticular space. Although it is assumed that these large syncitia were hypertrophic (and fused) phagocytes, it cannot be ruled out that the giant cells can also form direct infection of spongy connective tissue cells. Giant cell development appears to mirror that which occurs in other xenoma forming Microsporidia such as *Glugea* spp. where macrophages transport parasites to the site of giant cell formation but actual origin of the giant cell is less clear (e.g. Sánchez et al., 2001; Rodríguez-Tovar et al., 2003; Lom and Dykova, 2005).

Leitch et al. (2005) proposed that for giant cell formation to occur, the host cell must be capable of continuous mitosis and not be differentiated. In this context, despite debate over whether haemocytes released from the hematopoietic tissues retain proliferative capacity (see Johansson et al., 2000), several studies have reported the presence of mitotic figures in circulating crustacean haemocytes (e.g. Gargioni and Barracco, 1998). Whereas the proportion of circulating cells undergoing division is typically less than 1%, in cases of bacterial or fungal infection, this number increased to 3%, indicating that division in circulating cells may be at least partly responsible for the elevated haemocyte count associated with certain infections (Sequeira et al., 1996). Although, Johnson (1980) states that mitotic figures have not been noted in spongy connective tissues, she does record the presence of bi-nucleate cells (especially in post-moult crabs), suggesting that the spongy connective tissue cells are able to undergo mitotic division. The spongy connective tissues of crustaceans are also rich in mitochondria and glycogen (Johnson, 1980). Taken together, the potential for haemocytes (phagocytes), and spongy connective tissue cells, to replicate provides at least a basis for giant cell formation (associated with *A. rohanae* infection) to occur in both cell lineages. Regardless of their origin, the fused syncitia observed in histology were consistent with the large white cysts observed externally in infected crabs in processing facilities and these cysts are therefore a useful diagnostic feature for distinguishing infected crabs. Further studies are necessary to define the specific origin of the giant cell in *A. rohanae* infections of *L. santolla*.

Spores of *A. rohanae* were ornamented by characteristic bristles, the formation of which was apparently initiated during late merogony and early sporogony. Development of these bristles occurred in a zone between the multinucleate meront wall and the inner SPV wall. Sporogony was marked by apparent migration of tubular bristles to the surface of the exospore layer of the (early) sporoblast. In the mature spore, the exospore became multi-layered and covered with a dense mat of bristles, apparently rooted within the endosporal or exosporal layers. Such ornamentation has been described for numerous other microsporidium genera including Ameson Sprague, 1977, Annecalia Issi et al., 1993, Hirsutosporos Battson, 1983, Janecekia Larsson, 1983, Larssonella Weiser and David, 1997, Ringueletium Garcia, 1990, Tabanispora Bykova et al., 1987, and Trichoctospora Larsson, 1994. In other genera (including Tuzetia Maurand et al., 1971, Trichotuzetia Vavra et al., 1997, and Nudisporea Larsson, 1990), fibrils or tubules formed during sporogony connect the inner wall of the SPV to the sporont/sporoblast wall and are inherited by the mature spore. In their comprehensive review, Vávra and Lukeš (2013) propose that spore ornamentation is most evident in Microsporidia infecting aquatic hosts (or those with an aquatic phase in their life cycle) and as such, may aid transmission by increasing buoyancy of the spore and maximising time in the water column. At present, although *per os* transmission has been demonstrated for other Microsporidia infecting marine crustaceans

(e.g. *Ameson michaelis*, Overstreet, 1978), we know nothing of the transmission capacity of *A. rohanae* or the potential for alternative hosts to occur within its life cycle. Basic studies to investigate potential for crab-crab transmission are required in order to elucidate potential for spread of infection in the fishery, or in post-capture holding scenarios.

## Acknowledgments

The authors acknowledge funding support of DG SANCO of the European Commission under Cefas contact #C5839 (to GDS) and to the UK Department for Environment, Food and Rural Affairs (Defra) under Cefas contract #FB002 (to SWF) for completion of this work.

## References

- Balbiani, E.G., 1882. Sur les microsporidies ou psorospermies des articules. C.R. Acad. Sci. Paris. Ser. D 95, 1168–1171.
- Bancroft, J.D., Stevens, A., 1996. Theory and Practice of Histological Techniques. Churchill Livingstone, Pearson Professional Ltd, UK, pp. 99–112.
- Batson, B.S., 1983. A light and electron microscopic study of *Hirsutosporos austrosimulii* gen. n., sp. n. (Microspora: Nosematidae), a parasite of *Austrosimulium* sp. (Diptera, Simuliidae) in New Zealand. Protistologica 19, 263–280.
- Brown, A.M.V., Adamson, M.L., 2006. Phylogenetic distance of *Thelohania butleri* Johnston, Vernick, and Sprague, 1978 (Microsporidia; Thelohaniidae), a parasite of the smooth pink shrimp *Pandalus jordani*, from its congeners suggests need for a major revision of the Genus *Thelohania* Henneguy, 1892. J. Eukaryot. Microbiol. 53, 445–455.
- Bykova, H.I., Sokolova, Y.Y., Issi, I.V., 1987. Ultrastructural peculiarities of sporogonial stages of *Tabanispora bacillifera* gen. n. from tabanids. Abstract IV Congr. Parasitol. Leningrad. p. 20.
- Capella-Gutiérrez, S., Marçet-Houben, M., Gabaldón, T., 2012. Phylogenomics supports microsporidia as the earliest diverging clade of sequenced fungi. BMC Biol. 10, 47. <http://dx.doi.org/10.1186/1741-7007-10-47>.
- Chatton, E., Courrier, R., 1923. Formation d'un complexe xénoparasitaire géant avec bordure en brosse, sous l'influence d'une Microsporidie, dans le testicule de *Cottus bimaculatus*. C. R. Soc. Biol. (Paris) 89, 579–583.
- Donaldson, W.E., Byersdorfer, S.C., 2005. Biological field techniques for lithodid crabs. Alaska Sea Grant Program, University of Alaska Fairbanks. AK-SG-05-03, p. 76.
- Debaisieux, P., 1931. Études cytologiques du *Mrazekia argoisi*. Cellule 40, 147–168.
- Fitch, W.M., 1971. Towards defining the course of evolution: minimum change for a specific tree topology. Syst. Zool. 20, 406–416.
- Freeman, M.A., Bell, A.S., Sommerville, C., 2003. A hyperparasitic microsporidian infecting the salmon louse, *Lepeophtheirus salmonis*: an rDNA-based molecular phylogenetic study. J. Fish Dis. 26, 667–676.
- Garcia, J.J., 1990. Un nuevo microsporidio patógeno de larvas de simulodos (Diptera: Simuliidae) Ringuleum pilosa gen. et sp. nov. (Microspora, Caudosporidae). Neotropica 36, 111–122.
- Gargioni, R., Barracco, M.A., 1998. Hemocytes of the palaemonids *Macrobrachium rosenbergii* and *M. acanthurus*, and of the penaeid *Penaeus paulensis*. J. Morphol. 236, 209–221.
- Hazard, E.I., Oldacre, S.W., 1975. Revision of the Microsporidia (Protozoa) close to *Thelohania* with descriptions of one new family, eight new genera and thirteen new species. USDA Tech. Bull. 1530, 104 pp.
- Hopwood, D., 1996. Theory and practice of histopathological techniques, fourth ed. In: Bancroft, J.D., Stevens, A. (Eds.), Fixation and Fixatives. Churchill Livingstone, Hong Kong, pp. 23–46.
- Issi, I.V., Krylova, S.V., Nikolaeva, V.M., 1993. The ultrastructure of the microsporidian *Nosema meligethi* of the new genus Annicalia. Parazitologiya 27, 127–131.
- Johansson, M.W., Keyser, P., Sritunyalucksana, K., Soderhall, K., 2000. Crustacean haemocytes and haematozois. Aquaculture 191, 45–52.
- Johnson, P.T., 1980. Histology of the Blue Crab, *Callinectes sapidus*: A Model for the Decapoda. Praeger Publishers, New York.
- Larsson, R., 1983. A revisionary study of the taxon *Tuzetia* Maurand, Fize, Fenwick and Michel, 1971, and related forms (Microspora, Tuzetiidae). Protistologica 19, 323–355.
- Larsson, J.I.R., 1990. Description of a new microsporidium of the water mite *Limnochares aquatica* and establishment of the new genus *Napamiculum* (Microspora, Thelohaniidae). J. Invertebr. Pathol. 55, 152–161.
- Larsson, J.I.R., 1994. *Trichocostosporea pygopellita* gen. et sp. nov. (Microspora: Thelohaniidae), a microsporidian parasite of the mosquito *Aedes vexans* (Diptera, Culicidae). Arch. Protistenkd. 144, 147–161.
- Leitch, G.J., Shaw, A.P., Colden-Stanfield, M., Scanlon, M., Visvesvara, G.S., 2005. Multinucleate host cells induced by *Vittaforma corneae* (Microsporidia). Folia Parasitol. 52, 103–110.
- Lom, J., Dykova, I., 2005. Microsporidian xenomas in fish seen in wider perspective. Folia Parasitol. 52, 69–81.
- Matthews, R.A., Matthews, B.F., 1980. Cell and tissue reaction of turbot *Scophthalmus maximus* L. to *Tetramicra brevifilum* (Microspora). J. Fish Disease 3, 495–51.
- Maurand, J., Fize, A., Fenwick, B., Michel, R., 1971. Études au microscope électronique de *Nosema infirmum* Kudo, 1921, microsporidie parasite d'un copépode cyclopoidé; création du genre nouveau *Tuzetia* à propos de cette espèce. Protistologica 7, 221–225.
- Mrázek, A., 1899. Sporozenostudien II. Glugea lophii Doflein. Sitzungsber. Böh. Ges. Wiss. Math.-Naturwiss. Classe: 1–8.
- Morado, J.F., 2011. Protistan diseases of commercially important crabs: a review. J. Invertebr. Pathol. 106, 27–53.
- Overstreet, R.M., 1978. Marine maladies?: Worms, germs, and other symbionts from the northern Gulf of Mexico. Mississippi-Alabama Sea Grant, Program. p. 140.
- Reynolds, E.S., 1963. The use of lead citrate at high pH as an electron-opaque stain in electron microscopy. J. Cell Biol. 17, 208–212.
- Rodríguez-Tovar, F.J., Wright, G.M., Wadowska, D.W., Speare, D.J., Markham, R.J.F., 2003. Ultrastructural study of the late stages of *Loma salmonae* development in the gills of experimentally infected rainbow trout. J. Parasitol. 89, 464–474.
- Ryazanova, T.V., Eliseikina, M.G., 2010. Microsporidia of the genera *Thelohania* (Thelohaniidae) and *Ameson* (Perezziidae) in two species of lithodid crabs from the Sea of Okhotsk. Russ. J. Mar. Biol. 36, 435–442.
- Sánchez, J.G., Speare, D.J., Markham, R.J.F., Wright, G.M., Kibenge, F.S.B., 2001. Localization of the initial developmental stages of *Loma salmonae* in rainbow trout (*Oncorhynchus mykiss*). Vet. Pathol. 38, 540–546.
- Schröder, O., 1909. Thelohania chaetogastris, eine neue in Chaetogaster diaphanus Grünth schmarotzende Microsporidienart. Arch. Protistenkd. 14, 119–133.
- Sequeira, T., Tavares, D., Arala-Chaves, M., 1996. Evidence for circulating hemocyte proliferation in the shrimp *Penaeus japonicus*. Dev. Comp. Immunol. 20, 97–104.
- Sprague, V., 1977. Annotated list of species of microsporidia. In: Bulla, L.E., Cheng, T.C. (Eds.), Comparative Pathobiology, vol. 2. Plenum Press, New York, USA, pp. 31–334.
- Stentiford, G.D., Bateman, K.S., Small, H.J., Moss, J., Shields, J.D., Reece, K.S., Tuck, I., 2010. *Myospora metanephrops* (n. gen., n. sp.) from marine lobsters and a proposal for erection of a new Order and Family (Crustacea; Myosporidae) in the Class Marinospordia (Phylum Microsporidia). Int. J. Parasitol. 40, 1433–1446.
- Stentiford, G.D., Bateman, K.S., Dubuffet, A., Stone, D., 2011. *Hepatospora eriocheir* (Wang & Chen, 2007) gen. et comb. nov. from European Chinese mitten crabs (*Eriocheir sinensis*). J. Invertebr. Pathol. 108, 156–166.
- Stentiford, G.D., Bateman, K.B., Feist, S.W., Chambers, E., Stone, D.M., 2013a. Plastic parasites: extreme dimorphism creates a taxonomic conundrum in the phylum Microsporidia. Int. J. Parasitol. 43, 339–352.
- Stentiford, G.D., Bateman, K.S., Feist, S.W., Stone, D.M., Dunn, A.M., 2013b. Microsporidia: diverse, dynamic and emergent pathogens in aquatic systems. Trends Parasitol. <http://dx.doi.org/10.1016/j.pt.2013.08.005>.
- Tamura, K., Dudley, J., Nei, M., Kumar, S., 2007. MEGA4: molecular evolutionary genetics analysis (MEGA) software version 4.0. Mol. Biol. Evol. 24, 1596–1599.
- Thompson, J.D., Gibson, T.J., Plewniak, F., Jeanmougin, F., Higgins, D.G., 1997. The CLUSTAL\_X windows interface: flexible strategies for multiple sequence alignment aided by quality analysis tools. Nucleic Acids Res. 25, 4876–4882.
- Tourtip, S., Wongtripop, S., Sritunyalucksana, K., Stentiford, G.D., Bateman, K.S., Sriurairatana, S., Chayaburakul, K., Chavadej, K., Wityachumarnkul, B., 2009. *Enterocytozoon hepatopenaei* sp. nov. (Microspora: Enterocytozoonidae), a parasite of the black tiger shrimp *Penaeus monodon* (Decapoda: Penaeidae): fine structure and phylogenetic relationships. J. Invertebr. Pathol. 102, 21–29.
- Vavra, J., Larsson, J.I.R., Baker, M.D., 1997. Light and electron microscopic cytology of *Trichotuzetia guttata* gen. et sp. n. (Microspora, Tuzetiidae), a microsporidian parasite of *Cyclops vicinus* Ulanjin, 1875 (Crustacea, Copepoda). Arch. Protistenkd. 147, 293–306.
- Vávra, J., Lukeš, J., 2013. Microsporidia and “the art of living together”. Adv. Parasitol. 82, 254–319.
- Vossbrinck, C.R., Debrunner-Vossbrinck, B.A., 2005. Molecular phylogeny of the Microsporidia: ecological, ultrastructural and taxonomic considerations. Folia Parasitol. 52, 131–142.
- Wang, T.C., Nai, Y.S., Wang, C.Y., Solter, L.F., Hsu, H.C., Wang, C.H., Lo, C.F., 2013. A new microsporidium, *Triwangia caridinae* gen. nov., sp. nov. parasitizing fresh water shrimp, *Caridina formosae* (Decapoda: Atyidae) in Taiwan. J. Invertebr. Pathol. 112, 281–293.
- Weissenberg, R., 1949. Cell growth and cell transformation induced by intracellular parasites. Anat. Rec. 103, 517–518.
- Weiser, J., David, L., 1997. A light and electron microscopic study of *Larssoniella resinella* n. gen., n. sp. (Microspora, Unikaryonidae), a parasite of *Petnova resinella* (Lepidoptera, Tortricidae) in Central Europe. Arch. Protistenkd. 147, 405–410.